



## Research article

Effect of photocatalytic Fe<sub>2</sub>O<sub>3</sub> nanoparticles on urban runoff pollutant removal by permeable concrete

Rosangel Ortega-Villar<sup>a,b</sup>, Liliana Lizárraga-Mendiola<sup>c</sup>, Claudia Coronel-Olivares<sup>a</sup>, Luis D. López-León<sup>c</sup>, Carlos Alfredo Bigurra-Alzati<sup>c</sup>, Gabriela A. Vázquez-Rodríguez<sup>a,\*</sup>

<sup>a</sup> Área Académica de Química, Universidad Autónoma Del Estado de Hidalgo, Km. 4.5 Carr. Pachuca-Tulancingo, Cd. Universitaria, 42067, Mineral de La Reforma Hgo, Mexico

<sup>b</sup> Universidad Politécnica de Pachuca, Km. 20 Carr. Pachuca-Cd. Sahagún, Ex-Hacienda de Santa Bárbara, 43830, Zempoala Hgo, Mexico

<sup>c</sup> Área Académica de Ingeniería y Arquitectura, Universidad Autónoma Del Estado de Hidalgo, Km. 20 Carr. Pachuca-Cd. Sahagún, Ex-Hacienda de Santa Bárbara, 43830, Zempoala Hgo, Mexico

## ARTICLE INFO

## Keywords:

Low-impact development  
Nonpoint pollution control  
Disinfection  
Stormwater quality enhancement

## ABSTRACT

Permeable pavements are an efficient urban runoff (UR) management solution that also improve water quality. In this work, a photocatalytic layer of Fe<sub>2</sub>O<sub>3</sub> nanoparticles (NP) was incorporated into permeable concrete to evaluate its impact on the removal of several microbiological (*Escherichia coli*, *Pseudomonas aeruginosa*, *Aeromonas hydrophila*, and *Enterococcus faecalis*) and physicochemical (N-NH<sub>4</sub><sup>+</sup>, N-NO<sub>3</sub><sup>-</sup>, phenol, PO<sub>4</sub><sup>3-</sup>, Fe, Mn, and Pb) pollutants. First, permeable concrete samples were created with sufficient compressive strength and hydraulic conductivity for light traffic. The test samples were then coated with a mixture containing either 3% or 5% Fe<sub>2</sub>O<sub>3</sub> NP by cement weight. Control samples were prepared without NP. Scanning electron microscopy, energy dispersive spectroscopy, and X-ray photoelectron spectroscopy analyses showed that the nanoparticles remained unaltered on the concrete's surface. Synthetic URs simulating the microbiological or physicochemical composition of real UR were applied to the samples to evaluate their pollutant removal efficiencies. The depollution performances of the test (with 3% and 5% Fe<sub>2</sub>O<sub>3</sub> NP) and control samples were statistically compared. The test samples (3% NP, 5% NP, and the controls) significantly modified ( $p < 0.05$ ) most of the measured variables (i.e., the concentrations of *E. coli*, *A. hydrophila*, PO<sub>4</sub><sup>3-</sup>, Fe, Mn, and Pb) in the synthetic URs. Unexpectedly, the test samples (with 3% or 5% Fe<sub>2</sub>O<sub>3</sub> NP) did not significantly remove ( $p > 0.05$ ) some pollutants prone to oxidation, such as phenol or ammonium. However, the 5% NP sample significantly enhanced Mn removal. In general, the decontamination performances of the concrete samples with Fe<sub>2</sub>O<sub>3</sub> NP were not influenced by the nanoparticles; thus, they did not appear to add value to the generated permeable concrete. Nevertheless, our results indicate the considerable benefits of implementing permeable concrete to improve the quality of UR.

## 1. Introduction

Urban runoff (UR) has become an issue caused by urban expansion and local increases in the area of impervious surfaces. UR modifies watershed hydrology through the generation of excessive peak flows, channel alterations, and soil erosion, and is also a prominent nonpoint pollution source. In industrialized countries, UR is the main factor affecting the quality of fresh and coastal water (Abdollahian et al., 2018).

Low-impact development (LID) promotes an urbanization approach that integrates land and water management (Jiang et al., 2015). The goal of LID is to reestablish the predevelopment hydrological conditions through the implementation of devices such as bioretention cells, green

roofs, and permeable pavements. These devices can effectively reduce UR volume and soil erosion while improving UR quality (Shafique and Kim, 2017).

Permeable pavements are a relatively new alternative to conventional pavements, which constitute approximately 25% of impervious urban surfaces (Mullaney and Lucke, 2014). The different permeable pavements include block pavers, plastic grid systems, porous asphalt, and porous concrete. Permeable pavements are the most-used LID devices in developed countries (Shafique and Kim, 2017) as they do not require an increase in the land area. Furthermore, they can be added to UR treatment trains in a relatively simple manner and at a considerably lower cost than conventional stormwater drain systems (Jiang et al.,

\* Corresponding author.

E-mail address: [gvazquez@uaeh.edu.mx](mailto:gvazquez@uaeh.edu.mx) (G.A. Vázquez-Rodríguez).

<https://doi.org/10.1016/j.jenvman.2019.04.104>

Received 30 November 2018; Received in revised form 24 April 2019; Accepted 25 April 2019

Available online 07 May 2019

0301-4797/© 2019 Elsevier Ltd. All rights reserved.

2015). These pavements are reportedly the most effective LID practice for controlling rainfall events below 2 cm and can reduce runoff rates of 50–93% (Shafique and Kim, 2017).

Permeable pavements are also useful for removing common pollutants, such as total suspended solids (58–96%), total nitrogen (58–81%), and heavy metals (Cu, 15–95%; Pb, 25–99%; Zn, 40–98%), from UR (Shafique and Kim, 2017; Drake et al., 2013; Imran et al., 2013). Their ability to remove microbiological pollutants has received less attention than their physicochemical pollutant removal efficiency during evaluation. However, it has been demonstrated that permeable pavements can significantly reduce UR microbiological pollution (Abdollahian et al., 2018).

Several mechanisms are responsible for the pollutant removal by permeable pavements. Particulate matter can be trapped by mechanical filtration or sedimentation through the pavement, but dissolved pollutants can also be removed by sorption, precipitation, or biologically mediated processes (Drake et al., 2013), including the biodegradation of organic compounds and nitrogen transformation processes, such as nitrification (Tota-Maharaj and Scholz, 2010).

The addition of a photocatalytic layer to permeable pavements is a recent technique that has been proposed to decrease both air and water pollution in urban areas. The catalyst, usually nano-sized  $\text{TiO}_2$ , is first activated by ultraviolet radiation ( $< 390 \text{ nm}$ ). This material oxidizes organic and inorganic compounds through the production of active oxygen species, such as hydroxyl radicals ( $\cdot\text{OH}$ ) or superoxide ions ( $\text{O}_2^-$ ) (Tota-Maharaj and Coleman, 2017). Photocatalytic permeable pavements have mostly been used as a highly efficient purification device against air pollutants, such as  $\text{NO}_x$ ,  $\text{SO}_x$ ,  $\text{NH}_3$ ,  $\text{CO}$ , volatile aromatic hydrocarbons, and polycyclic aromatic hydrocarbons (Asadi et al., 2012; Hassan et al., 2012). However, nanoscale  $\text{TiO}_2$  may not be suitable as it could damage ecosystems and human health (Zhu et al., 2012).

Iron oxide nanostructures are widespread in terrestrial and aquatic environments. In soils, a global budget of  $10^5 \text{ Tg}$  of iron oxide nanoparticles (NP) has been estimated (Guo and Barnard, 2013). The weathering of iron-bearing minerals or the action of microorganisms, birds, social insects, and even humans can form these nanostructures. Excluding hematite, most iron oxides exist as nanobiomaterials in living organisms (Guo and Barnard, 2013). Several iron oxide nanostructures have been proposed as photocatalysts for the degradation of organic pollutants. Although they often have low activity or their activity easily declines, some of these materials can absorb visible light in addition to light in the UV wavelength range (Xu et al., 2012).

This study investigates the effects of a photocatalytic iron oxide ( $\text{Fe}_2\text{O}_3$ ) NP layer on the removal of common UR pollutants, including several microbial indicators and physicochemical pollutants, by permeable concrete (PC). PC samples were produced and characterized using scanning electron microscopy (SEM), energy dispersive spectroscopy (EDS), and x-ray photoelectron spectroscopy (XPS).

## 2. Materials and methods

### 2.1. Development of the PC samples

Based on previous research (Ortega-Villar et al., 2017), a PC formula for roads with light traffic, pedestrian areas, and bikeways, was selected to evaluate its ability to decontaminate UR. To decrease variability, all PC samples were simultaneously produced from the same batch of cement and aggregate source. We used ordinary Portland cement type I, and its physical properties and chemical composition followed the ASTM C150-07 standard (ASTM, 2007). The coarse aggregate complied with ASTM size 67 (12.5–10 mm) (ASTM, 2011a), while the small coarse aggregate complied with ASTM 88 (9.5–4.75 mm) (ASTM, 2018). The water/cement ratio was 0.4, while the coarse aggregate/cement ratio was 3.64. The sample preparation method has been described elsewhere (Ortega-Villar, 2017). Triplicate samples were soaked

in distilled water at room temperature (around  $21^\circ\text{C}$ ) and cured for 7, 14, and 28 days according to ASTM C192/C192M-16a to evaluate their compressive strength (ASTM, 2016). Only the samples cured for seven days were used for the remaining analyses and tests. After curing, the samples were left to dry at room temperature for at least 48 h.

A mixture of  $\text{Fe}_2\text{O}_3$  NP, cement, sand, and water was applied to the surface of each dry test sample. Commercially available (Sigma-Aldrich™, USA) crystalline  $\text{Fe}_2\text{O}_3$  nanoparticles (CAS: 1309-37-1, primarily  $\gamma$ ,  $< 50 \text{ nm}$ ) were used at contents of 3% or 5% by cement weight. The sand was sieved to remove particles smaller than  $300 \mu\text{m}$  and increase the porosity of the coating (Hassan et al., 2012). The constituents were mixed at the following ratios according to the description provided by Ortega-Villar (2017): 0.03 or 0.05 nanoparticles and 1:3.8:0.6 of cement, sand, and water, respectively. The 3% and 5% NP mixtures were applied separately to two batches of two samples using a dry brush. Prior to application, the surface was roughened with sandpaper to improve the mixture's adhesion. The two blank samples were coated with a mixture similar to that used above, however, it contained 3% soil instead of nanoparticles. The coated samples were kept covered at room temperature for at least 48 h before being used in the experiments.

### 2.2. Characterization of the PC samples

To assess the compressive strength and hydraulic conductivity of the PC, samples were prepared with certain sizes from the same batches of materials with the formulations described above. The compressive strength of cylinders (15 and 30 cm in diameter and height, respectively) with curing times of 7, 14, and 28 days was measured in triplicate (Controls, model 50-C43C04, Milan, Italy). The average strength of these three samples was calculated for each stage of curing.

One 7 cm-thick square sample with an area of  $225 \text{ cm}^2$  was produced to determine the hydraulic conductivity using Eq. (1) (ASTM, 2011b).

$$k = \frac{L * \left(\frac{Q}{t}\right)}{(A * \Delta H)} \quad (1)$$

where  $k$  is the hydraulic conductivity, m/s;  $L$  is the length of the sample, m;  $Q/t$  is the water flow rate,  $\text{m}^3/\text{s}$ ;  $A$  is the cross-sectional area of the sample,  $\text{m}^2$ ; and  $\Delta H$  is the constant hydraulic head value, m, required to maintain a certain flow rate,  $Q/t$ . The water flow rate was determined in triplicate by measuring the volume of water collected in a water recipient over time. The samples were previously sealed with a waterproof film to prevent water from flowing in through the sides.

After curing and coating with 3% and 5% of NP, the test samples were fully immersed in deionized water for 24 h and dried for another 24 h at room temperature (around  $21^\circ\text{C}$ ). A small fraction of each sample (5 g) was obtained from the surface and analyzed by energy dispersive spectrometry (EDS)-x-ray microanalysis and x-ray photoelectron spectroscopy (XPS). A Thermo JEOL electron microscope (model JSM-6300, Akishima, Japan) that can conduct high-resolution morphological observation (3.0–4.0 nm) was used for the EDS x-ray microanalysis. XPS was conducted using a Thermo Scientific K-Alpha x-ray photoelectron spectrometer (Waltham, MA, USA) operated at 150 W with Al  $\text{K}\alpha$  as the exciton source ( $h\nu = 1486.6 \text{ eV}$ ).

### 2.3. Preparation of synthetic urban runoffs

To evaluate the microbial pollutant removal, four microbiological urban runoffs (MURs) were prepared separately with known concentrations (target values) of each microbial indicator, including *Escherichia coli* ATCC 11229 ( $3 \log_{10} \text{ CFU/mL}$ ), *Pseudomonas aeruginosa* ATCC 10145 ( $7 \log_{10} \text{ CFU/mL}$ ), *Aeromonas hydrophila* ATCC 49140 ( $5 \log_{10} \text{ CFU/mL}$ ), and *Enterococcus faecalis* ATCC 14506 ( $3 \log_{10} \text{ CFU/mL}$ ). To the best of our knowledge, neither *P. aeruginosa* nor *A.*

*Aeromonas hydrophila* have been used to evaluate the performance of permeable pavements.

The target values were selected after reviewing the concentrations of these microbial indicators for urban runoff or rainwater reported in literature. The concentration ranges of *E. coli*, *P. aeruginosa*, *Enterococcus* sp., and *Aeromonas* sp. ( $\log_{10}$  CFU/mL) found in literature were  $-0.92$ – $4.3$  (Grebel et al., 2013; Selvakumar and Borst, 2006; Makepeace et al., 1995);  $0.53$ – $5.04$  (Selvakumar and Borst, 2006; Makepeace et al., 1995);  $0.08$ – $3.58$  (Sidhu et al., 2012; Makepeace et al., 1995); and  $0.96$ – $3.21$  (the latter was reported for *Aeromonas* sp. in rainwater collected in a rain barrel; Shuster et al., 2013), respectively.

A full description of the bacterial culture preparation method is given in Ortega-Villar (2017). In short, each strain was cultured separately in trypticase soy agar and incubated at  $37^\circ\text{C}$  for 24 h. After incubation, some colonies were cultured in 250 mL of a trypticase soy broth. The absorbance of each microbial suspension at 550 nm was measured and used to estimate the microbial concentration according to the 0.5 McFarland scale. The estimated concentration of each microbial indicator was adjusted to the target value with a sterile saline solution (0.7% of NaCl).

Another synthetic urban runoff (PUR) sample was prepared to simulate the physicochemical composition of the UR sampled in our location (Pachuca City, Hgo., Mexico; Ortiz-Hernández et al., 2016). Concentrated solutions of several chemicals ( $\text{NH}_4\text{Cl}$ ,  $\text{KNO}_3$ , phenol,  $\text{KH}_2\text{PO}_4$ ,  $\text{FeCl}_3$ ,  $\text{MnSO}_4$ , and  $\text{PbNO}_3$ ) were added to commercial bottled water at known quantities to achieve the concentrations of  $\text{N-NH}_4^+$  (2 mg/L),  $\text{N-NO}_3^-$  (2 mg/L), chemical oxygen demand (COD, 50 mg/L), dissolved orthophosphates ( $\text{PO}_4^{3-}$ , 3 mg/L), Fe (15 mg/L), Mn (0.3 mg/L), and Pb (0.5 mg/L) measured in the real UR generated at the study site (Ortega-Villar, 2017).

#### 2.4. Evaluation of pollutant removal by the PC samples

For all tests, a rain event was defined as the application of 500 mL of synthetic runoff (MUR or PUR) to a PC sample at a constant rate for 1 h through a peristaltic pump. MUR or PUR was evenly distributed over the surface of each sample by an electric ventilator. Rain events on each PC sample (3% NP, 5% NP, and the control) were simulated five times in successive runs. Prior to each run, each sample was irradiated with light at a wavelength of 365 nm for 60 min for activation (Yu, 2003). Fig. 1 shows the experimental setup.

The applied water volume was equivalent to a total rainfall of 212 mm, which was the maximum monthly rainfall recorded for Pachuca City from 1951 to 2010 (SMN, 2017). Although the rainfall regime varies greatly per month, this rain event closely represents the maximum rainfall level and extreme conditions in terms of both the runoff quantity and the concentration of each pollution indicator. These extreme conditions are likely to be experienced in the study zone at the beginning of the rainy season, when a seasonal first-flush effect results in high pollution loads due to the length of the preceding dry period (Ortiz-Hernández et al., 2016).

Microbial pollutant removal by the PC samples (coated with 3% or 5%  $\text{Fe}_2\text{O}_3$  NP and a control) was evaluated separately for each microbial indicator (*E. coli*, *P. aeruginosa*, *A. hydrophila*, and *E. faecalis*). Each synthetic MUR was prepared under sterile conditions and applied to the samples as described above. Samples were collected in triplicate from the inlet and the outlet after the end of each UR application, and analyzed by the techniques described in the following section. Physicochemical pollutant removal was evaluated under the same conditions using the synthetic PUR described in section 2.3.

#### 2.5. Analytical techniques

Unless indicated otherwise, the parameters were measured in triplicate according to standard methods (APHA, 2012). The

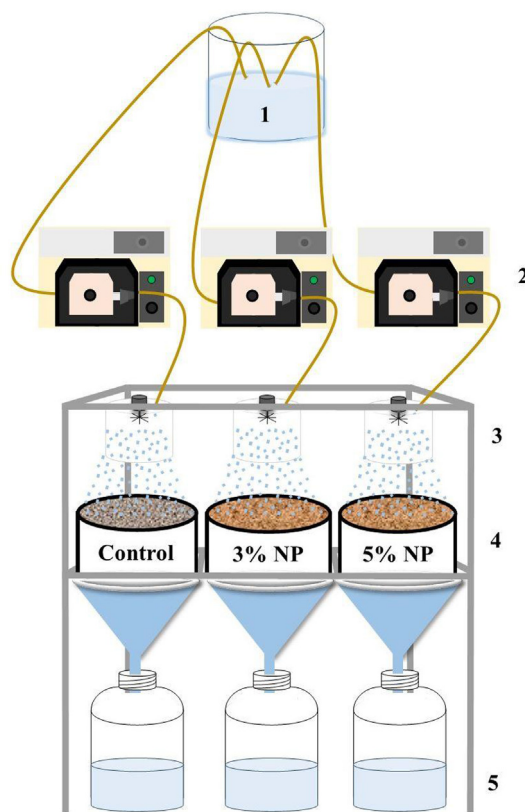


Fig. 1. Laboratory setup simulating the application of urban runoff to the permeable concrete specimens. 1: Inflow storage tank; 2: Peristaltic pumps; 3: Mechanical ventilators; 4: Permeable concrete specimens; 5: Outflow storage tanks.

microbiological indicators were measured following plate count techniques. Serial decimal dilutions of the MUR samples were plated onto Petri dishes with selective agar. The Petri dishes were then incubated for 18–24 h at  $35 \pm 2^\circ\text{C}$ , unless stated otherwise. The use of m-FC agar (Sigma-Aldrich™, St. Louis, USA) allowed the measurement of *E. coli* after incubation for 22–24 h at  $44.5$ – $45.5^\circ\text{C}$ . *Pseudomonas* agar (BD DIFCO™, Maryland, USA) was used to assess the quantity of *P. aeruginosa*, while selective agars supplied by OXOID™ (Hampshire, England) and BD DIFCO™ (Maryland, USA) were used for *A. hydrophila* and *E. faecalis*, respectively. The microbiological results were expressed as the  $\log_{10}$  values (CFU/mL). The  $\text{N-NH}_4^+$  (phenate method, 4500-NH<sub>3</sub> F),  $\text{N-NO}_2^-$  (method 4500-NO<sub>2</sub><sup>-</sup> B),  $\text{N-NO}_3^-$  (Mubarak et al., 1977), COD (method 5220 D), and  $\text{PO}_4^{3-}$  (method 4500-P E) concentrations were measured in PUR samples. Metals (Fe, Mn, and Pb) were analyzed by atomic absorption spectrometry (AAS) using a Varian 800 spectrometer (PerkinElmer, USA).

#### 2.6. Data analyses

The log removal values of the indicator microorganisms were calculated based on the  $\log_{10}$  CFU/mL differences between the inlet and outlet samples. The removal of the physicochemical variables was calculated as a percentage. Box plots were produced to examine the differences in the removal ( $\log_{10}$  removal or percentage of removal) achieved by each PC sample (3% NP, 5% NP and the control). The data were statistically analyzed to compare the concentration values in MUR or PUR before and after passing through the PC samples (3% NP, 5% NP and the control). The statistical tests were performed for the microbial indicators after the data were log-transformed. The normality of the data (or log-transformed data) was verified using the skewness values. Two-sided paired Tukey tests with a 95% confidence level were

conducted to determine the statistical significance of the changes in the pollutant concentrations after passing through the PC samples. All statistical tests were conducted using Minitab 16 (Minitab Inc., State College, PA, USA).

### 3. Results and discussion

#### 3.1. Characterization of the PC samples

The average compressive strengths of the PC samples after curing for 7, 14, and 28 days were 5.2, 6.9, and 8.39 MPa, respectively. According to some authors (Lim et al., 2013; Lian et al., 2011), these values can be considered low. However, they are within the ranges established for permeable pavements used for light traffic (3.4–27.4 MPa) (Aire, 2011). The average hydraulic conductivity (*k*) was 360 mm/min, which is also adequate for a permeable pavement (Winston et al., 2016). This property can vary widely based on the particle size of the PC, or the shape and degree of connectivity of the pores (Turco et al., 2017). Therefore, some authors have stated that the hydraulic conductivity should be high to avoid pore saturation (Valeo and Gupta, 2018).

Fig. 2 presents SEM images of the surface morphology of the samples coated with 3% and 5% Fe<sub>2</sub>O<sub>3</sub> NP. Note that the surface of the sample with 5% NP (Fig. 2b) was more homogeneous than that of the 3% NP sample (Fig. 2a). The EDS analysis of the PC coated with 3% and 5% Fe<sub>2</sub>O<sub>3</sub> NP (Fig. 2a and b, respectively) indicated that the contents of O, Al, K, Fe, Zn, Mg, and Ca in the 5% Fe<sub>2</sub>O<sub>3</sub> NP sample were higher than those in the 3% NP sample. The results presented in Fig. 2b (5%

Fe<sub>2</sub>O<sub>3</sub> NP) confirmed that the ratios of iron and oxygen were greater than those of the sample coated with 3% Fe<sub>2</sub>O<sub>3</sub> NP (Fig. 2a). According to the results presented above, the 5% NP sample seems more suitable for removing pollutants through photooxidation than the 3% NP sample.

XPS can provide qualitative and quantitative information about the chemical elements present on a sample's surface. The incidence of a photon on the surface atoms causes the emission of photoelectrons that can be characterized by their binding energy (measured in eV). As elements typically exhibit different characteristic binding energies, these binding energies can be used to identify the elements to which each peak corresponds (Palomino-Reséndiz et al., 2017).

Fig. 3 presents the XPS spectra obtained from the outer surface of the 3% and 5% NP samples. Both spectra were similar due to the positions of the Fe2p<sub>3/2</sub> (723 eV) and Fe2p<sub>1/2</sub> (711.10 eV) peaks, which corresponded to oxidized iron (Fe<sup>3+</sup>). Moreover, in both spectra, the Fe2p<sub>3/2</sub> peak was narrower and more intense than the Fe2p<sub>1/2</sub> peak. A satellite peak of Fe2p<sub>3/2</sub> was located at 718.4 eV, which also indicated the presence of Fe<sup>3+</sup> (Palomino-Reséndiz et al., 2017). These results, along with the SEM-EDS results, verified the unaltered presence of Fe<sub>2</sub>O<sub>3</sub> on the PC samples.

#### 3.2. Evaluation of the microbial pollutant removal by the PC samples

Fig. 4 shows the microbial pollutant removal efficiencies of the PC samples (in log units). *Escherichia coli* was completely removed from the synthetic MUR as it was undetected in the filtrates of the three samples. This corresponded to removal values of 2.613–4.303 log<sub>10</sub> (CFU/mL).

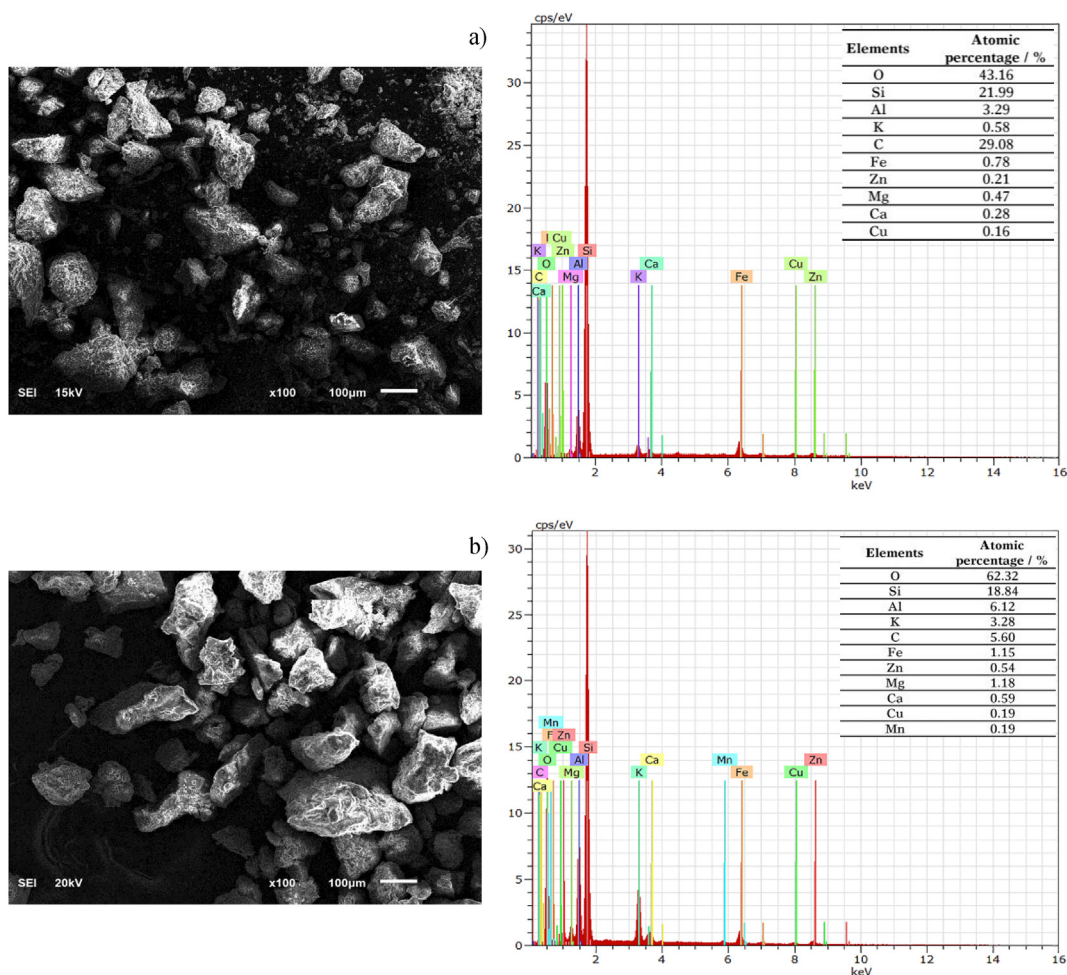


Fig. 2. SEM and EDS spectra images of the permeable concrete specimens: a) 3% Fe<sub>2</sub>O<sub>3</sub> NP and b) 5% Fe<sub>2</sub>O<sub>3</sub> NP.

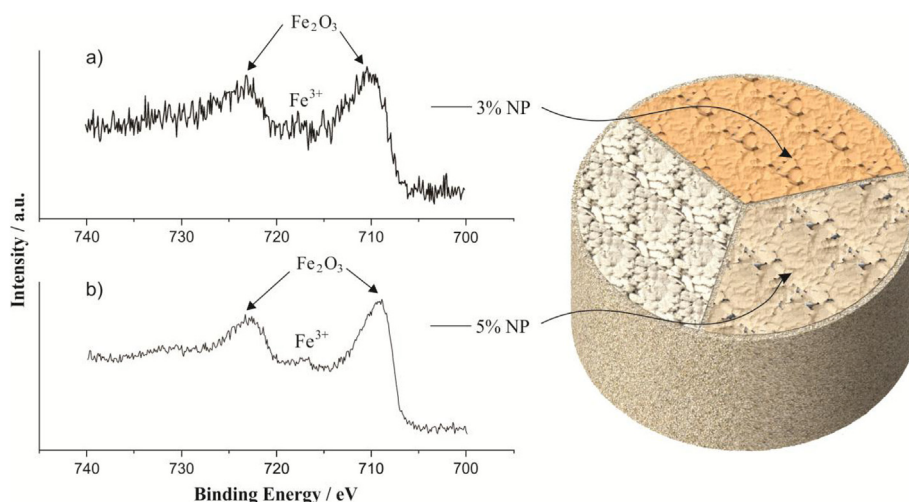


Fig. 3. General XPS spectra obtained from the outer surface of the permeable concrete specimens: a) 3% Fe<sub>2</sub>O<sub>3</sub> NP and b) 5% Fe<sub>2</sub>O<sub>3</sub> NP.

*Aeromonas hydrophila* was also completely removed by the three samples. For this microorganism, the log<sub>10</sub> removal values were higher (2.564–10.533) than those for *E. coli* as the initial concentrations introduced to the synthetic UR were also greater. The initial *E. coli* and *A. hydrophila* concentrations were significantly different (in all cases, *p* = 0.000) from those measured in the filtrates of each sample.

The removal of *P. aeruginosa* and *E. faecalis* by the PC samples were more variable than the *E. coli* and *A. hydrophila* removal performances (Fig. 4). The log<sub>10</sub> removal values of *P. aeruginosa* ranged from 0 to 4.973, which corresponded to elimination efficiencies between 0 and 99.99%. The only significant difference (*p* = 0.003) between the initial and final concentration of this indicator was observed after the MUR passed through the 3% NP sample. The log<sub>10</sub> removal values of *E. faecalis* were between 0.115 and 1.054 (equivalent to a range of 36–91%). The samples did not significantly modify the concentration of this indicator (*p* = 0.435, 0.072, and 0.222 for the control, 3% NP, and 5% NP samples, respectively). Regardless of which PC sample was tested, both *P. aeruginosa* and *E. faecalis* were detected in all outlet samples.

*Escherichia coli* is the most widely used microorganism for studying the performance of LID systems. Therefore, the comparisons with other permeable pavement-based studies were limited to this microbial

indicator. In a previous study, a removal performance of 3.5–4.5 log<sub>10</sub> (CFU/mL) was reported for permeable pavement combined with a geothermal heat pump. This system considerably reduced the concentration of *E. coli* (98.6%) (Tota-Maharaj and Scholz, 2010). However, in our study, the removal efficiency of this organism was always 100%.

The removal of *E. coli* reported here and in other studies based on pervious pavements (as Tota-Maharaj and Scholz, 2010) appears to be more significant than that achieved by other LID technologies. Elimination efficiencies of approximately 90% (average log<sub>10</sub> removal of 2.0) have been reported for *E. coli* and for fecal coliforms in biofilters in general (Li et al., 2012). This level of depollution has also been achieved in non-vegetated biofilters, where the upper layer is responsible for most of the removal of bacteria (Zhang et al., 2011). As *E. coli* is smaller than the pores of typical filtering materials, straining and sorption have been proposed as the main removal mechanisms during filtration (Kim et al., 2012). These mechanisms occur in pervious concrete and likely explain the high removal rates of *E. coli* and *A. hydrophila* achieved by our samples. The elimination of *E. coli* and *Enterococcus* spp. by other LID technologies, such as wetlands (not relying on filtration), is much lower (53% and 61%, respectively) (Jiang et al., 2015).

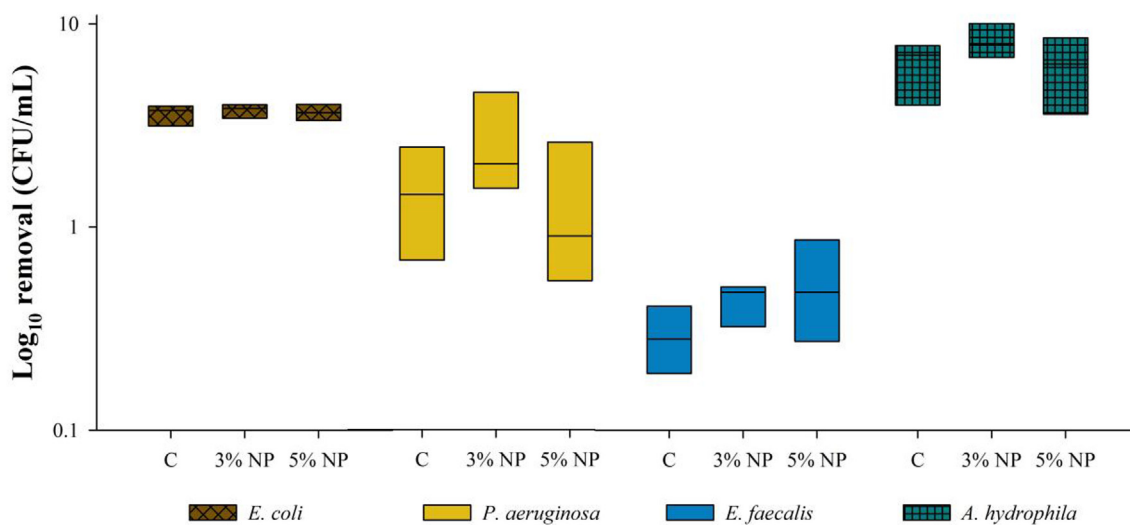


Fig. 4. Efficiencies of the permeable concrete specimens at removing *Escherichia coli*, *Pseudomonas aeruginosa*, *Enterococcus faecalis*, and *Aeromonas hydrophila*. C: Control specimen; 3% NP: specimen-coated by 3% of Fe<sub>2</sub>O<sub>3</sub> nanoparticles; 5% NP: specimen-coated by 5% of Fe<sub>2</sub>O<sub>3</sub> nanoparticles. Box plots show medians and 10th and 90<sup>th</sup> percentiles.

As described above and in Fig. 4, the efficiency of the PC samples varied depending on the microbial indicator. This result agrees with previous literature, which indicates that microbial transport through porous media is affected by the surface charge, hydrophobicity, size, mobility and shape of the cells, as well as their physiological state and membrane type (i.e., whether they are Gram-positive or negative) (Park et al., 2010; Mitik-Dineva et al., 2009; Smets et al., 1999). As these factors vary between microbial species, the removal rate of a PC might differ depending on the studied microorganism.

Several of *E. coli*'s characteristics constrain its movement through porous media, thereby enhancing its removal. The surface of *E. coli* cells is more hydrophobic and adhesive than that of other pathogenic organisms, such as *Staphylococcus aureus* (Park et al., 2010). In addition, the rod shape and size of *E. coli* hinder its transport in porous environments when compared to smaller and spherical bacteria. Finally, *E. coli* is Gram-negative and motile, which enhance cell adhesion to solid media (Park et al., 2010). These characteristics are shared with *A. hydrophila*, which is morphologically indistinguishable from *E. coli* (Percival and Williams, 2014). The similarity of their shapes could explain the similar removal efficiencies for both bacteria in this study.

*Pseudomonas aeruginosa* exhibits some of the features listed above, such as its motility and Gram-negative and rod-shaped characteristics, allowing it to adhere to solid media. However, in our experiments, the removal efficiency of *P. aeruginosa* was lower than that of *E. coli* and *A. hydrophila*. The low retention in the PC samples could be due to the lower electronegativity of the cell surface of *P. aeruginosa* than that of *E. coli* (Mitik-Dineva et al., 2009) if the available surface of our PC samples was positively charged, however, this is unknown.

*Enterococcus faecalis* is expected to be poorly retained by porous media as it is nonmotile, Gram-positive, and spherical (Park et al., 2010), and this was confirmed by its elimination rates, which were lowest among the studied indicators. The mean *E. faecalis* elimination rate of the three PC samples was 0.425 log<sub>10</sub> CFU/mL, which is similar to that of enterococci reported for a sand biofilter (0.36 log<sub>10</sub> CFU/mL; Peng et al., 2016). Other studies report the low *E. faecalis* removal efficiency of filtration-based systems. For instance, Chen and Walker (2012) eliminated 89% of *E. coli* and 15% of *E. faecalis* using sand columns. Consequently, *E. faecalis* appears to be a stringent indicator of the microbial pollutant removal efficiency of LID systems.

### 3.3. Evaluation of the physicochemical pollutant removal efficiency of the PC samples

Fig. 5 shows the organic matter and nutrient removal efficiencies of the PC samples. The nitrate ion removal efficiencies are not presented in Fig. 5 as no removal was observed. The concentrations of this pollutant were always higher in the filtrates than those in the PUR. After passing through the PC, the increases in the nitrate concentration ranged from 78.0 to 142.8% (control sample), 53.3–133.3% (3% NP sample), and 54–104% (5% NP sample). According to previous studies, permeable pavements often increase the nitrate concentrations in the field (Abdollahian et al., 2018; Shafique and Kim, 2017).

Nitrite ions were not added to the PUR, but they were detected in the outlets at the following concentrations: 0.07–0.095 mg/L (control sample), 0.09–0.12 mg/L (3% NP sample), and 0.06–0.11 mg/L (5% NP sample). The inlet concentrations of N-NO<sub>2</sub><sup>-</sup> and N-NO<sub>3</sub><sup>-</sup> were significantly different ( $p = 0.000$  in all cases) to the concentrations measured at the outlet of the three samples. The emergence of nitrite and nitrate in the PC filtrates may be linked to the oxidation of ammonium, which has been observed in other studies. For instance, Drake et al. (2014) reported the elimination of ammonium (81–87%) and nitrite (62–82%) ions in runoff, along with a net augmentation of nitrate (13–140%) after filtration through three permeable pavements. According to the authors, this was due to biologically mediated ammonium oxidation (i.e., nitrification).

In our study, the mean removal efficiencies of N-NH<sub>4</sub><sup>+</sup> were 21.8,

27.5, and 37.4% for the control, 3% NP, and 5% NP samples, respectively. However, the initial N-NH<sub>4</sub><sup>+</sup> concentrations were not significantly different from those in the filtrates of each ( $p = 0.268, 0.166,$  and  $0.082$  for the control, 3% NP, and 5% NP samples, respectively). Our removal rates were similar to those reported for ammonium in previous studies. For example, Abdollahian et al. (2018) reported ammonium removal rates of 45.9% and 17.3% at two different permeable pavement sites. Li et al. (2017) observed an initial N-NH<sub>4</sub><sup>+</sup> removal rate of approximately 35%, which was explained by ion exchange with the monovalent cations (Na<sup>+</sup> and K<sup>+</sup>) commonly found in PC materials. In our tests, the decrease in ammonium was accompanied by increases in nitrite and nitrate with an almost stoichiometric relationship after only 1 h of contact. The short contact time indicates that the likely removal mechanism was chemical oxidation, rather than microbial nitrification.

COD removal was highly variable for each sample. The initial COD concentrations were not significantly different from those measured in the filtrates of the NP-coated concrete samples ( $p = 0.153$  and  $0.142$  for the 3% NP and 5% NP samples, respectively). However, the values at the inlets to the control sample were significantly different ( $p = 0.048$ ) to those at the outlets. The control sample achieved an average COD removal efficiency of 46.6%, which was similar to the removal efficiencies achieved by the 3% and 5% NP samples (45.6 and 45.3%, respectively). In a recent study, COD removal efficiencies of 66 and 39% were obtained for porous asphalt and concrete samples when glucose was used as the model organic pollutant (Li et al., 2017). Glucose is less adsorbable than phenol (Elmabrouk, 2008), however, Li et al. attributed the removal of glucose to adsorption on available surfaces.

In our assays, the samples collected at the outlets of the three samples were slightly yellow in color. This change in color could be due to the *meta* cleavage of catechol, an intermediate of phenol degradation, which forms 2-hydroxymuconic acid semialdehyde, a yellow-colored compound (Vázquez-Rodríguez et al., 2006). The *meta* cleavage of phenol is a common biodegradation pathway of this compound, suggesting that active phenol-degrading bacteria colonized the three PC samples. However, this needs to be addressed through further studies. Catechol is commonly reported as an intermediate of phenol photo-oxidation, along with resorcinol, 1,2,3-benzenetriol, and hydroquinone. The cleavage of these compounds produces malonic acid and, subsequently, short-chain organic acids, but not 2-hydroxymuconic acid semialdehyde. Ultimately, these organic acids transform into CO<sub>2</sub> and H<sub>2</sub>O (Ahmed et al., 2010).

The inlet concentrations of phosphates significantly differed from the concentrations measured at the outlets of the three samples ( $p = 0.000$  in all cases). High PO<sub>4</sub><sup>3-</sup> removal rates (94.3%, 95.8%, and 94.3%) were achieved by the control, 3% NP, and 5% NP samples, respectively (Fig. 5). High removal efficiencies are often reported in the bibliography for this pollutant: Drake et al. (2014) reported efficiencies between 9 and 82% at real permeable pavement sites, Vázquez-Rivera et al. (2015) reported efficiencies exceeding 90% in PC supplemented with fly ash and magnetite nanoparticles, and Kim et al. (2017) reported a removal efficiency of approximately 98% in PC composed by calcium sulfoaluminate cement and coal bottom ash aggregates. Phosphate removal by permeable pavements can follow several mechanisms. Filtration removes particulate phosphates, while geochemical adsorption removes dissolved phosphates through adsorption and precipitation (Drake et al., 2014). Other authors have suggested that the precipitation of phosphates into hydroxyapatite (Ca<sub>10</sub>(PO<sub>4</sub>)<sub>6</sub>(OH)<sub>2</sub>) and amorphous calcium phosphate (Ca<sub>3</sub>(PO<sub>4</sub>)<sub>2</sub>) is the main removal mechanism in permeable pavements (Vázquez-Rivera et al., 2015).

Fig. 6 presents the metal removal rates. The PC samples significantly changed the concentrations of Fe, Mn, and Pb in the filtrates (in all cases,  $p = 0.000$ ). As expected, the removal rates of Fe and Pb were higher than those measured for Mn. In urban runoff, Mn is more associated with the dissolved phase than Fe and Pb, which are mostly found attached to particles (Nieber et al., 2014). The tendency of Fe and

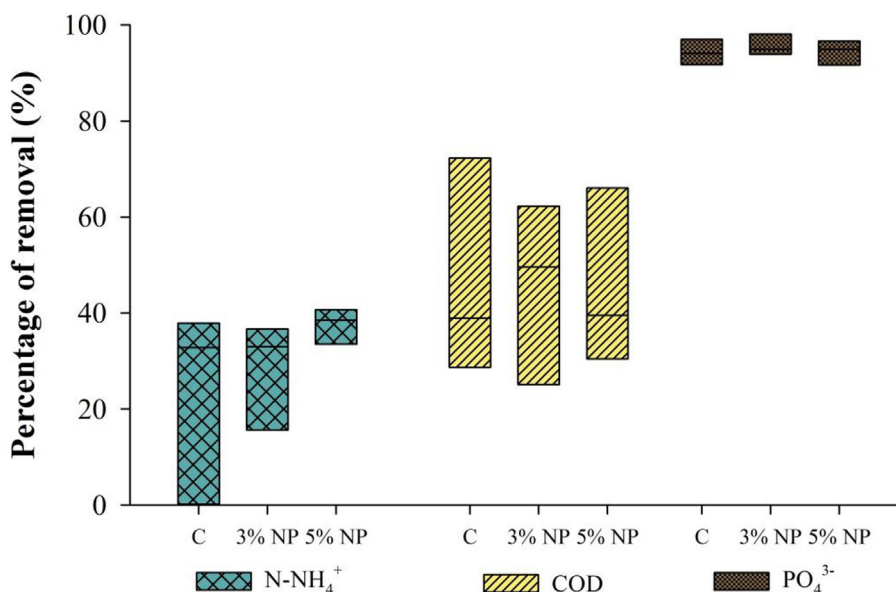


Fig. 5. Efficiencies of the permeable concrete specimens at removing N-NH<sub>4</sub><sup>+</sup>, chemical oxygen demand (COD), and PO<sub>4</sub><sup>3-</sup>. C: Control specimen; 3% NP: specimen-coated by 3% of Fe<sub>2</sub>O<sub>3</sub> nanoparticles; 5% NP: specimen-coated by 5% of Fe<sub>2</sub>O<sub>3</sub> nanoparticles. Box plots show medians and 10th and 90<sup>th</sup> percentiles.

Pb to adsorb to solids agrees with the high removal rates achieved by the PC samples, which could have mainly occurred by adsorption.

The mean Fe removal rates were 83.3, 84.0, and 87.7% for the control, 3% NP, and 5% NP samples, respectively. Drake et al. (2014) reported Fe removal efficiencies ranging from 32% to 74% in an onsite survey of three permeable pavement systems. Furthermore, Abdollahian et al. (2018) observed mean dissolved iron reduction efficiencies of 60.2%.

The mean Mn removal rates measured in our tests were 48.8, 46.0, and 58.7% for the control, 3% NP, and 5% NP samples, respectively. Pervious concrete pavers with grass swale have achieved Mn removal rates exceeding 75% (Imran et al., 2013). Lead is measured more

frequently than manganese and iron as an indicator of the performance of permeable pavements owing to its prevalence in UR and its potential risk to human health. The Pb elimination rates of our control, 3% NP, and 5% NP samples were 73.1%, 76.8%, and 78.4%, respectively. The average removal efficiencies of lead by permeable pavements varies significantly; Drake et al. (2014) reported efficiencies of 25–93%, while Shafique and Kim (2017) reported efficiencies of 40–99%. In his review, Scholz (2014) concluded that pervious pavements can reduce lead concentrations at efficiencies reaching 79% and cause lead to become undetectable.

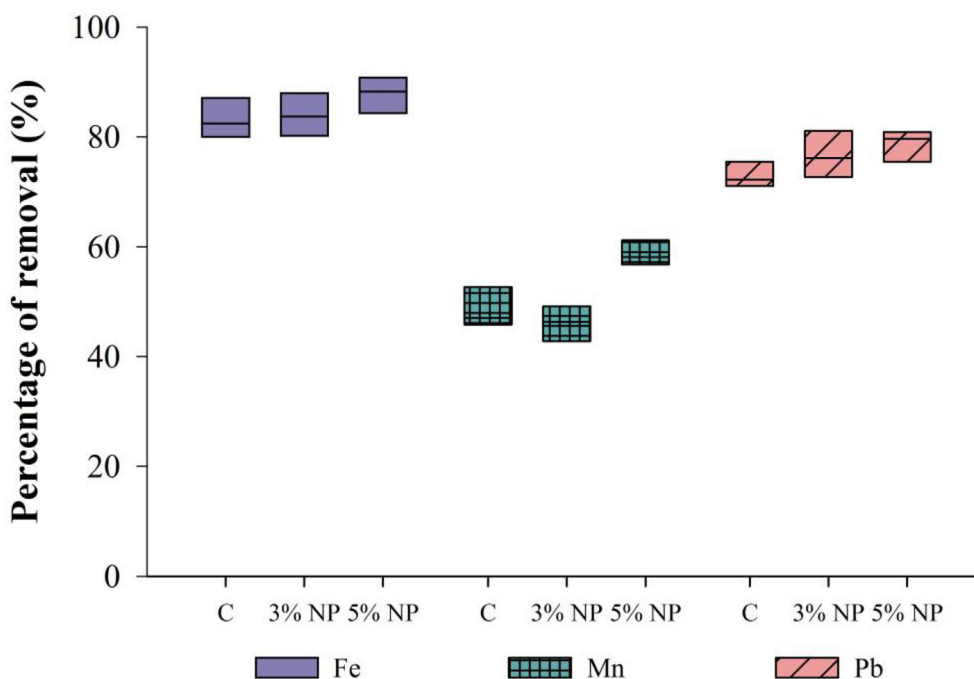


Fig. 6. Efficiencies of the permeable concrete specimens at removing Fe, Mn, and Pb. C: Control specimen; 3% NP: specimen-coated by 3% of Fe<sub>2</sub>O<sub>3</sub> nanoparticles; 5% NP: specimen-coated by 5% of Fe<sub>2</sub>O<sub>3</sub> nanoparticles. Box plots show medians and 10th and 90<sup>th</sup> percentiles.

### 3.4. Effect of Fe<sub>2</sub>O<sub>3</sub> NP on pollutant removal by the PC samples

For each water quality variable, all the concentrations measured at the inlets to the three samples in the tests were compared to those at the outlets using Tukey tests ( $p < 0.05$ ). The concentrations of the microbial indicators were first log-transformed. For all variables, significant differences were found between the inlets to the three samples and the outlets. Thus, the PC significantly modified ( $p < 0.05$ ) the quality of the inflow, regardless of the presence and quantity of Fe<sub>2</sub>O<sub>3</sub> NP.

The paired comparisons of the removal efficiencies for most of the analyzed parameters (log<sub>10</sub> removal efficiencies for microbial indicators) did not exhibit any differences between the three samples (Tukey tests, 95% confidence level). Several studies have reported the effect of NP photocatalytic activity on cell structures, which often causes microbial inactivation or lysis (Regmi et al., 2018). However, in our experiments, the Fe<sub>2</sub>O<sub>3</sub> NP did not enhance the removal of the studied microbial indicators or other pollutants prone to oxidation, such as phenol or NH<sub>4</sub>, by the PC.

The manganese removal efficiency presented the only exception to the absence of differences between samples. The efficiency of the 5% NP sample was significantly different ( $p = 0.000$ ) to that achieved by the 3% NP and control samples. These results suggest that the Fe<sub>2</sub>O<sub>3</sub> NP in the 5% sample promoted the removal of dissolved Mn<sup>2+</sup> by oxidation, to a certain extent. Once formed, the sample would have retained the solid Mn oxide. Mn oxidation is kinetically hindered in the absence of a promoter. However, bacteria or solid surfaces commonly accelerate oxidation in many natural systems. Nanoscale hematite first adsorbs dissolved Mn<sup>2+</sup> and then donates electrons, thereby encouraging oxidation (Madden and Hochella, 2005).

## 4. Conclusions

PC samples with adequate hydraulic conductivity and compressive strength for light traffic were prepared. The samples were coated with Fe<sub>2</sub>O<sub>3</sub> nanoparticles (3% and 5%), which remained unaltered on the concrete surfaces, as indicated by the SEM-EDS and XPS analyses. The designed concrete mix improved the quality of synthetic urban runoff, as most of the measured variables (i.e., *E. coli*, *A. hydrophila*, PO<sub>4</sub><sup>3-</sup>, Fe, Mn, and Pb) were significantly modified ( $p = 0.000$ ) after passing through the created samples (3% NP, 5% NP, and the control). *Enterococcus faecalis* appeared as a stringent indicator of the disinfection efficiency, as this bacterium was not significantly removed by any of the tested PC samples. The nitrate concentrations increased and nitrites appeared in the filtrates after short contact with the samples, indicating the abiotic oxidation of ammonium rather than biological nitrification. The test samples coated with Fe<sub>2</sub>O<sub>3</sub> NP did not significantly reduce ( $p > 0.05$ ) the concentrations of organic matter (phenol) or ammonium. It was unclear whether phenol underwent chemical or biological oxidation.

Further research should be undertaken to determine which of the removal mechanisms occurred in the PC samples. However, the role of Fe<sub>2</sub>O<sub>3</sub> NP in improving the depollution efficiency of PC may be limited under the tested conditions. The three samples exhibited similar performances that were independent of the presence of nanoparticles, and Fe<sub>2</sub>O<sub>3</sub> NP may have only influenced Mn removal by the 5% NP samples.

Our findings could encourage the further implementation of PC in the field. The urban runoff quality was improved by our PC formulation, which is economical and easy to replicate. Future work could explore the pollutant removal efficiency of other naturally occurring nanoscale oxides (Fe<sub>3</sub>O<sub>4</sub> and MnO<sub>2</sub>, among others) or oxyhydroxides in LID technologies.

## Declarations of interest

None.

## Acknowledgments

We thank David Felipe Paz Casas (Laboratory of Materials Resistance, UAEH) for the kind assistance with the elaboration of the permeable concrete specimens. We owe special thanks to Dr. Juan Carlos Flores-Segura (RIP) for his invaluable help with the SEM-EDS and XPS analyses. This research did not receive any specific grant from funding agencies in the public, commercial, or not-for-profit sectors.

## References

- Abdollahian, S., Kazemi, H., Rockaway, T., Gullapalli, V., 2018. Stormwater quality benefits of permeable pavement systems with deep aggregate layers. *Environments* 5, 68. <https://doi.org/10.3390/environments5060068>.
- Ahmed, S., Rasul, M.G., Martens, W.N., Brown, R., Hashib, M.A., 2010. Heterogeneous photocatalytic degradation of phenols in wastewater: a review on current status and developments. *Desalination* 261, 3–18. <https://doi.org/10.1016/j.desal.2010.04.062>.
- Aire, C., 2011. Concreto permeable: alternativa sustentable. *Constr. Tecnol. Concr.* 3 [in Spanish]. <http://www.imcyc.com/revistacyt/jun11/arttecnologia.htm>, Accessed date: 23 April 2019.
- APHA, 2012. *Standard Methods for the Examination of Water and Wastewater*, twenty-second ed. American Public Health Association/American Water Works Association/Water Environment Federation, Washington D.C., USA.
- Asadi, S., Hassan, M., Keven, J., Rupnow, T., 2012. Development of photocatalytic pervious concrete pavement for air and storm water improvements. *Transport. Res. Rec.* 2290, 161–167. <https://doi.org/10.3141/2290-21>.
- ASTM, 2007. ASTM C150-07 Standard Specification for Portland Cement. ASTM International, West Conshohocken, PA. <https://doi.org/10.1520/C0150-07>.
- ASTM, 2011. ASTM C33/C33M-11a Standard Specification for Concrete Aggregates. ASTM International, West Conshohocken, PA. [https://doi.org/10.1520/C0033\\_C0033M-11A](https://doi.org/10.1520/C0033_C0033M-11A).
- ASTM, 2011. ASTM D4511-11 Standard Test Method for Hydraulic Conductivity of Essentially Saturated Peat. ASTM International, West Conshohocken, PA. <https://doi.org/10.1520/D4511-11>.
- ASTM, 2016. ASTM C192/C192M-16a Standard Practice for Making and Curing Concrete Test Specimens in the Laboratory. ASTM International, West Conshohocken, PA. [https://doi.org/10.1520/C0192\\_C0192M-16A](https://doi.org/10.1520/C0192_C0192M-16A).
- ASTM, 2018. ASTM C88/C88M-18 Standard Test Method for Soundness of Aggregates by Use of Sodium Sulfate or Magnesium Sulfate. ASTM International, West Conshohocken, PA. [https://doi.org/10.1520/C0088\\_C0088M-18](https://doi.org/10.1520/C0088_C0088M-18).
- Chen, G., Walker, S.L., 2012. Fecal indicator bacteria transport and deposition in saturated and unsaturated porous media. *Environ. Sci. Technol.* 46, 8782–8790. <https://doi.org/10.1021/es301378q>.
- Drake, J.A., Bradford, A., Marsalek, J., 2013. Review of environmental performance of permeable pavement systems: state of the knowledge. *Water Qual. Res. J. Can.* 48 (3), 203–222. <https://doi.org/10.2166/wqrjc.2013.055>.
- Drake, J., Bradford, A., Van Seters, T., 2014. Stormwater quality of spring–summer–fall effluent from three partial-infiltration permeable pavement systems and conventional asphalt pavement. *J. Environ. Manag.* 139, 69–79. <https://doi.org/10.1016/j.jenvman.2013.11.056>.
- Elmabrouk, F., 2008. Removal of phenol and *m*-cresol from petrochemical wastewater using PAC additional in activated sludge system. In: *Proc. 1st International Petroleum Environment Conference*, Tripoli, Libya.
- Grebel, J.E., Mohanty, S.K., Torkelson, A.A., Boehm, A.B., Higgins, C.P., Maxwell, R.M., Nelson, K.L., Sedlak, D.L., 2013. Engineered infiltration systems for urban stormwater reclamation. *Environ. Eng. Sci.* 30, 437–454. <https://doi.org/10.1089/ees.2012.0312>.
- Guo, H., Barnard, A.S., 2013. Naturally occurring iron oxide nanoparticles: morphology, surface chemistry and environmental stability. *J. Mater. Chem. A* 1, 27–42. <https://doi.org/10.1039/C2TA00523A>.
- Hassan, M.M., Dylla, H., Mohammad, L.N., Rupnow, T., 2012. Methods for the application of titanium dioxide coatings to concrete pavement. *Int. J. Pavement Res. Technol.* 5, 12–20.
- Imran, H.M., Akib, S., Karim, M.R., 2013. Permeable pavement and stormwater management systems: a review. *Environ. Technol.* 34, 2649–2656. <https://doi.org/10.1080/09593330.2013.782573>.
- Jiang, Y., Yuan, Y., Piza, H., 2015. A review of applicability and effectiveness of low impact development/green infrastructure practices in arid/semi-arid United States. *Environments* 2, 221–249. <https://doi.org/10.3390/environments2020221>.
- Kim, M.H., Sung, C.Y., Li, M.H., Chu, K.H., 2012. Bioretention for stormwater quality improvement in Texas: removal effectiveness of *Escherichia coli*. *Separ. Purif. Technol.* 84, 120–124. <https://doi.org/10.1016/j.seppur.2011.04.025>.
- Kim, G.M., Jang, J.G., Khalid, H.R., Lee, H.K., 2017. Water purification characteristics of pervious concrete fabricated with CSA cement and bottom ash aggregates. *Constr. Build. Mater.* 136, 1–8. <https://doi.org/10.1016/j.conbuildmat.2017.01.020>.
- Li, Y.L., Deletic, A., Alcazar, L., Bratieres, K., Fletcher, T.D., McCarthy, D.T., 2012. Removal of *Clostridium perfringens*, *Escherichia coli* and F-RNA coliphages by stormwater biofilters. *Ecol. Eng.* 49, 137–145. <https://doi.org/10.1016/j.ecoleng.2012.08.007>.
- Li, H., Li, Z., Zhang, X., Li, Z., Liu, D., Li, T., Zhang, Z., 2017. The effect of different surface materials on runoff quality in permeable pavement systems. *Environ. Sci.*

- Pollut. Res. 24, 21103–21110. <https://doi.org/10.1007/s11356-017-9750-6>.
- Lian, C., Zhuge, Y., Beecham, S., 2011. The relationship between porosity and strength for porous concrete. *Constr. Build. Mater.* 25, 4294–4298. <https://doi.org/10.1016/j.conbuildmat.2011.05.005>.
- Lim, E., Tan, K.H., Fwa, T.F., 2013. Effect of mix proportion on strength and permeability of pervious concrete for use in pavement. *J. East. Asia Soc. Transport. Stud.* 10, 1565–1575. <https://doi.org/10.11175/easts.10.1565>.
- Madden, A.S., Hochella, M.F., 2005. A test of geochemical reactivity as a function of mineral size: manganese oxidation promoted by hematite nanoparticles. *Geochem. Cosmochim. Acta* 69, 389–398. <https://doi.org/10.1016/j.gca.2004.06.035>.
- Makepeace, D.K., Smith, D.W., Stanley, S.J., 1995. Urban stormwater quality: summary of contaminant data. *Crit. Rev. Environ. Sci. Technol.* 25, 93–139. <https://doi.org/10.1080/10643389509388476>.
- Mitik-Dineva, N., Wang, J., Truong, V.K., Stoddart, P., Malherbe, F., Crawford, R.J., Ivanova, E.P., 2009. *Escherichia coli*, *Pseudomonas aeruginosa*, and *Staphylococcus aureus* attachment patterns on glass surfaces with nanoscale roughness. *Curr. Microbiol.* 58, 268–273. <https://doi.org/10.1007/s00284-008-9320-8>.
- Mubarak, A., Howald, R.A., Woodriff, R., 1977. Elimination of chloride interferences with mercuric ions in the determination of nitrates by the phenoldisulfonic acid method. *Anal. Chem.* 49, 857–860. <https://doi.org/10.1021/ac50014a047>.
- Mullaney, J., Lucke, T., 2014. Practical review of pervious pavement designs. *Clean. - Soil, Air, Water* 42, 111–124. <https://doi.org/10.1002/clean.201300118>.
- Nieber, J.L., Arika, C.N., Lahti, L., Gulliver, J.S., Weiss, P.T., 2014. The Impact of Stormwater Infiltration Practices on Groundwater Quality. St. Anthony Falls Laboratory, University of Minnesota Digital Conservancy. <https://conservancy.umn.edu/handle/11299/169456>, Accessed date: 23 April 2019.
- Ortega-Villar, R., 2017. Urban Runoff Disinfection in a Photocatalytic Permeable Pavement. [in Spanish]. Undergraduate Thesis. Biotechnology Engineering, Universidad Politécnica de Pachuca, Mexico.
- Ortega-Villar, R., Coronel-Olivares, C., Lizárraga-Mendiola, L., Beltrán-Hernández, R.I., Lucho-Constantino, C.A., Vázquez-Rodríguez, G.A., 2017. Removal of micro-biological pollutants from urban runoff by photocatalytic permeable pavements [in Spanish]. *Rev. Ing. Bioméd. Biotecnol.* 1, 1–7.
- Ortiz-Hernández, J., Lucho-Constantino, C., Lizárraga-Mendiola, L., Beltrán-Hernández, R.I., Coronel-Olivares, C., Vázquez-Rodríguez, G., 2016. Quality of urban runoff in wet and dry seasons: a case study in a semi-arid zone. *Environ. Sci. Pollut. Res.* 23, 25156–25168. <https://doi.org/10.1007/s11356-016-7547-7>.
- Palomino-Reséndiz, R.L., Bolarín-Miró, A.M., Sánchez-De Jesús, F., Espinós-Manzorro, J.P., Cortés-Escobedo, C.A., 2017. Análisis de la relación  $Fe^{3+}/Sr^{2+}$  de nanopartículas de  $SrFe_{12}O_{19}$  mediante XPS y su efecto sobre las propiedades magnéticas [in Spanish]. *Tópicos Inv. Cien. Tierra Mat.* 4, 2–11.
- Park, S.J., Kim, S.B., Kim, K.W., 2010. Analysis of bacterial cell properties and transport in porous media. *J. Environ. Sci. Health A* 45, 682–691. <https://doi.org/10.1080/10934521003648867>.
- Peng, J., Cao, Y., Rippey, M.A., Afroz, A.R.M., Grant, S.B., 2016. Indicator and pathogen removal by low impact development best management practices. *Water* 8, 600. <https://doi.org/10.3390/w8120600>.
- Percival, S.L., Williams, D.D., 2014. *Aeromonas*. In: Percival, S.L., Yates, M.V., Williams, D.D., Chalmers, R., Gray, N. (Eds.), *Microbiology of Waterborne Diseases*, second ed. Elsevier, London, pp. 49–64.
- Regmi, C., Joshi, B., Ray, S.K., Gyawali, G., Pandey, R.P., 2018. Understanding mechanism of photocatalytic microbial decontamination of environmental wastewater. *Front. Chem.* 6, 33. <https://doi.org/10.3389/fchem.2018.00033>.
- Scholz, M., 2014. Permeable pavements and storm water management. In: Gopalakrishnan, K., Steyn, W., Harvey, J. (Eds.), *Climate Change, Energy, Sustainability and Pavements*. Green Energy and Technology. Springer, Berlin, Heidelberg, pp. 247–260.
- Selvakumar, A., Borst, M., 2006. Variation of microorganism concentrations in urban stormwater runoff with land use and seasons. *J. Water Health* 4 (1), 109–124. <https://doi.org/10.2166/wh.2006.0009>.
- Shafique, M., Kim, R., 2017. Green stormwater infrastructure with low impact development concept: a review of current research. *Desalin. Water Treat.* 83, 16–29. <https://doi.org/10.5004/dwt.2017.20981>.
- Shuster, W.D., Lye, D., La Cruz, A., Rhea, L.K., O'Connell, K., Kelty, A., 2013. Assessment of residential rain barrel water quality and use in Cincinnati, Ohio. *J. Am. Water Resour. Assoc.* 49, 753–765. <https://doi.org/10.1111/jawr.12036>.
- Sidhu, J.P.S., Hodgers, L., Ahmed, W., Chong, M.N., Toze, S., 2012. Prevalence of human pathogens and indicators in stormwater runoff in Brisbane, Australia. *Water Res.* 46, 6652–6660. <https://doi.org/10.1016/j.watres.2012.03.012>.
- Smets, B.F., Grasso, D., Engwall, M.A., Machinist, B.J., 1999. Surface physicochemical properties of *Pseudomonas fluorescens* and impact on adhesion and transport through porous media. *Colloids Surfaces B Biointerfaces* 14, 121–139. [https://doi.org/10.1016/S0927-7765\(99\)00030-2](https://doi.org/10.1016/S0927-7765(99)00030-2).
- SMN, 2017. Normales Climatológicas 1981-2000, Estación Pachuca, Hgo. [in Spanish]. Servicio Meteorológico Nacional, Comisión Nacional del Agua, Mexico.
- Tota-Maharaj, K., Scholz, M., 2010. Efficiency of permeable pavement systems for the removal of urban runoff pollutants under varying environmental conditions. *Environ. Prog. Sustain. Energy* 29, 358–369. <https://doi.org/10.1002/ep.10418>.
- Tota-Maharaj, K., Coleman, N., 2017. Developing novel photocatalytic cementitious permeable pavements for depollution of contaminants and impurities in urban cities. In: Proc. 10th International Conference on Environmental Engineering, Vilnius, Lithuania.
- Turco, M., Kodesová, R., Brunetti, G., Nikodem, A., Fér, M., Piro, P., 2017. Unsaturated behaviour of a permeable pavement: laboratory investigation and numerical analysis by using the HYDRUS-2D model. *J. Hydrol.* 554, 780–791. <https://doi.org/10.1016/j.jhydrol.2017.10.005>.
- Valeo, C., Gupta, R., 2018. Determining surface infiltration rate of permeable pavements with digital imaging. *Water* 10, 133–155. <https://doi.org/10.3390/w10020133>.
- Vázquez-Rivera, N.I., Soto-Pérez, L., St John, J.N., Molina-Bas, O.I., Hwang, S.S., 2015. Optimization of pervious concrete containing fly ash and iron oxide nanoparticles and its application for phosphorus removal. *Constr. Build. Mater.* 93, 22–28. <https://doi.org/10.1016/j.conbuildmat.2015.05.110>.
- Vázquez-Rodríguez, G., Ben Youssef, C., Waissman-Vilanova, J., 2006. Two-step modeling of the biodegradation of phenol by an acclimated activated sludge. *Chem. Eng. J.* 117, 245–252. <https://doi.org/10.1016/j.cej.2005.11.015>.
- Winston, R.J., Al-Rubaei, A.M., Blecken, G.T., Hunt, W.F., 2016. A simple infiltration test for determination of permeable pavement maintenance needs. *J. Environ. Eng.* 142 (10), 1–10. [https://doi.org/10.1061/\(ASCE\)EE.1943-7870.0001121](https://doi.org/10.1061/(ASCE)EE.1943-7870.0001121).
- Xu, P., Zeng, G.M., Huang, D.L., Feng, C.L., Hu, S., Zhao, M.H., Lai, C., Wei, Z., Huang, C., Xie, G.X., Liu, Z.F., 2012. Use of iron oxide nanomaterials in wastewater treatment: a review. *Sci. Total Environ.* 424, 1–10. <https://doi.org/10.1016/j.scitotenv.2012.02.023>.
- Yu, J.C., 2003. Deactivation and Regeneration of Environmentally Exposed Titanium Dioxide ( $TiO_2$ ) Based Products (Testing Report). Hong Kong, Environmental Protection Department, HKSAR.
- Zhang, L., Seagren, E.A., Davis, A.P., Karns, J.S., 2011. Long-term sustainability of *Escherichia coli* removal in conventional bioretention media. *J. Environ. Eng.* 137 (8), 669–677. [https://doi.org/10.1061/\(ASCE\)EE.1943-7870.0000365](https://doi.org/10.1061/(ASCE)EE.1943-7870.0000365).
- Zhu, Y., Eaton, J.W., Li, C., 2012. Titanium dioxide ( $TiO_2$ ) nanoparticles preferentially induce cell death in transformed cells in a Bak/Bax-independent fashion. *PLoS One* 7 (11), e50607. <https://doi.org/10.1371/journal.pone.0050607>.